Application of Electrical Resistivity Method with Peak and Flat Base Electrodes to Detect a Potential Water Leakage Underneath a Water Pool in Kiara Payung, Sumedang, West Java

M.N. Azizah[1], A.A. Valencia[1*], A. Kuswanto[2]

[1] Program Studi Geofisika, FMIPA, Universitas Indonesia, Kampus UI Depok, 16424, Indonesia

[2] PT Geoscan Eksplorasindo, Kota Bandung, Jawa Barat, 40611, Indonesia

*Corresponding author: ayunda.aulia@ui.ac.id

Abstract

The water pool at Kiara Payung Campsite, one of the largest campsites in West Java, Indonesia, is an important water storage facility that provides clean water for campers. However, this cuboid-shaped concrete structure is susceptible to leaks due to ground motion caused by earthquakes. Therefore, this study aims to detect potential leakage underneath the water pool using the electrical resistivity method with peak and flat base electrodes. Peak electrodes are unsuitable for hard materials like concrete as they can cause structural damage, while flat base electrodes can be used without compromising the integrity of the concrete. The study was performed using a single profile, employing various electrode combinations: all peak electrodes, a combination of peak and flat base electrodes, and all flat base electrodes. The profile length was 117.5 meters with 2.5 meters spacing between electrodes, utilizing a total of 48 electrodes. The measured apparent resistivity was inverted using the least-square and robust constraint inversion methods to obtain 2D true resistivity sections. An analysis of these 2D sections, model errors, and ability to delineate the water pool geometry, reveals that the robust constraint method with flat base electrodes provides the best result. This approach distinguishes the boundary between the water pool and surrounding soil, exhibits a smaller error, and accurately resolves the water pool geometry. These results indicate that no leakage is present beneath the water pool. Therefore, the electrical resistivity method using flat base electrodes is recommended for the maintenance of the water pool and other geoelectric studies on hard surfaces.

Keywords: electrical resistivity, peak electrode, flat base electrode, least-square, robust constraint inversion

1. Introduction

Kiara Payung is a camping ground located in Jatinangor, Sumedang, West Java, Indonesia, equipped with a concrete cuboid-shaped water pool for storing rainwater, which serves as the site's primary source of clean water. Given West Java's frequent tectonic activities (Supendi et al., 2018), regular pool maintenance is essential to assess potential leakage due to cracks in its concrete structure caused by ground motion from earthquakes. Since subsurface leakage is not visually detectable, geophysical methods, such as electrical resistivity, are recommended for maintenance. The electrical resistivity method, based on Ohm's Law, involves injecting electrical current into the earth using current electrodes and measuring the potential difference with potential electrodes to estimate subsurface resistivity (Loke, 1999). The distribution of resistivity in the subsurface can provide helpful information on soil saturation, indicating a potential leakage associated with the crack on the pool surface.

The electrical resistivity method has been widely used for geophysical investigations, such as groundwater search, archaeological study, and geothermal exploration (Chabaane et al., 2017; Karavul et al., 2016; Mohamaden et al., 2016; Riwayat et al., 2018). While this method has been used to detect leaks in buried water storage (Ramirez et al., 1996), it has not yet been applied to the study area. Conducting a resistivity survey on the water pool's concrete surface poses challenges, mainly when using peak electrodes. Previous studies have extensively tested the applicability of the flat base electrodes in various cases, such as the identification of chalky groundwater, void detection in the subsurface, detection of water supply tunnels, bedrock mapping, detection of abandoned shafts, investigation of road damage causes (Athanasiou et al., 2007; Zouhri & Lutz, 2010; Putra et al., 2020). In addition, flat base electrodes have also been used to identify subsurface anomaly models (Kurniawan et al., 2017) and on Roman mosaic floors (Carrara et al., 2001). These studies demonstrate that flat base electrodes can successfully provide resistivity profiles consistent with the field geometry. However, the applicability of the peak and flat base electrodes in detecting potential water leakage underneath a water pool requires further investigation.

Therefore, this study aims to investigate a potential water leakage underneath a water pool using peak and flat base electrodes. This study is performed in several steps. First, the electrical resistivity survey was conducted using a Wenner-Alpha configuration with three different electrode combinations (all peak electrodes, a combination of the peak and flat base electrodes, and all flat base electrodes). The Wenner-Alpha is suitable for shallow targets and sensitive to lateral changes (Reynolds, 1997; Adhe et al., 2022). Second, the measured apparent resistivity is inverted using least-square and robust constraint inversion methods. Last, a comparative analysis is performed between results obtained with different electrode combinations and inversion methods. This study can be used to show further the applicability of flat base electrodes in geophysical investigations.

2. Data and Method

2.1. Data

The data was obtained from Kiara Payung Campground, Sumedang, West Java. Data acquisition was conducted on 20 February 2023, with one profile traversing the water pool (Figure 1) using Ares 5A equipment and a 12V electronic power supply. The electrode spacing (a in equation 4) is 2.5 m, and the maximum n-separation between the electrodes (nmax in Figure 2) is 6. The profile length is 117.5 m. The main object of this study is the water pool made of concrete situated between profile lengths 62.5 m and 72.5 m. The current electrodes inject DC current 5A into the subsurface (I in equation 8), while the potential electrodes measure the potential difference (ΔV in equation 8) between these electrodes. The potential difference will be used to calculate the apparent resistivity of the subsurface (ρ_a in equation 8).

The topography profile in the study area shows a downward slope from Northwest to Southeast, with an elevation ranging from 952.5 to 960 meters above sea level (masl) (Figure 1). The water pool has an elevation of 957 masl, which has a rectangular shape with a width and length of 10.8 x 17.7 m^2 and a thickness of 2.15 m.

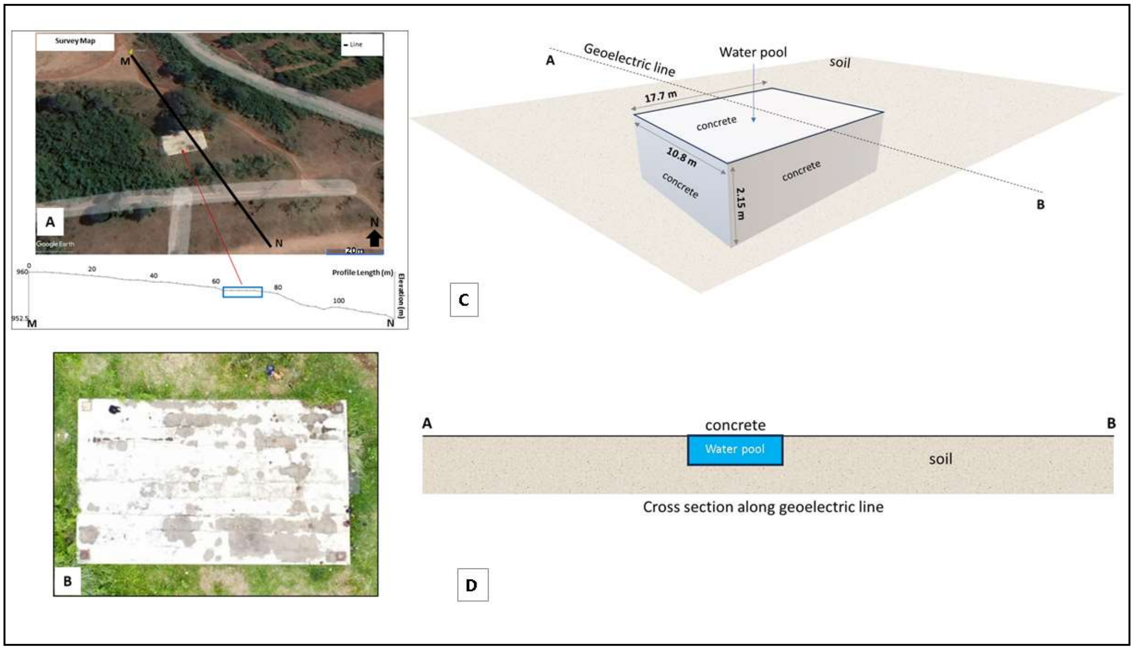

Figure 1. The survey area is at Kiara Payung, Sumedang, West Java (A). The electrical resistivity measurements were conducted using peak and/or flat base electrodes along the same profile depicted by the black line (see also Figure 4). The topography for this line is also shown. The location of the water pool is marked by a blue rectangular between profile lengths 62.5 m and 72.5 m. A close look at the water pool is also shown (B), which was taken from a drone. The well has a dimension of 17.7 m in length, 10.8 m in width, and 2.15 m in thickness. Sketch of water pool (C) and cross-section along survey line (D) shows the geometry of the water pool.

Three combinations of peak and flat base electrodes are used in this study (Figure 2). First, only peak electrodes are used, covering only the soil area, while no electrodes are positioned on the concrete surface of the well (Figure 2A). Second, peak electrodes are applied to the soil, whereas the flat base electrodes are on the concrete surface (Figure 2B). Third, only flat base electrodes cover the soil and the concrete surface (Figure 2C).

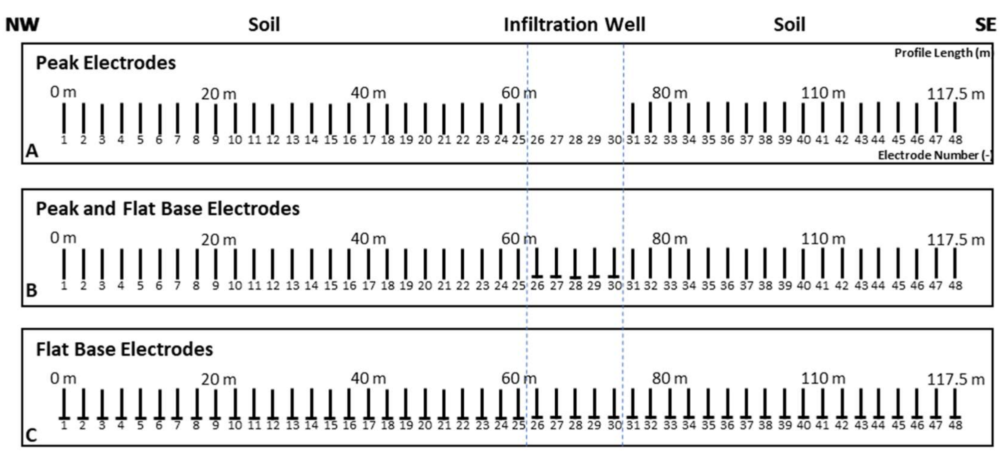

Figure 2. Peak and flat base electrodes are used in the electrical resistivity survey with three combinations: (A) all peak electrodes, (B) a combination of peak and flat base electrodes, and (C) all flat base electrodes. Vertical dotted blue lines mark the areal extent of the infiltration well (water pool).

2.2. Method

2.2.1. Electrodes

We use two types of electrodes in this survey: peak and flat base electrodes (Figure 3). Both electrode types have been used in previous studies (Athanasiou et al., 2007; Zouhri & Lutz, 2010; Putra et al., 2020). A peak electrode is a conventional electrode shaped like a long pipe with a pointed bottom end, measuring 0.4 m in length and 0.01 m in diameter (Figure 3A, C). The application of this electrode requires insertion into the soil, which leads to small contact resistance between the peak electrode and the soil due to soil moisture. In contrast, a flat base electrode is a new type of electrode with the shape of a square with a dimension of 0.1 m x 0.1 m and a thickness of 2 mm (Figure 3B, D). This electrode does not require insertion into the soil, allowing it to be used on a concrete surface. Both electrode types are made of iron.

Resistivity measurement using flat base electrodes on a concrete surface raises two issues. First, the coupling between the flat base electrodes and the concrete surface is low if the surface is not smooth. Second, the contact resistance is large because the surface is very dry (Athanasiou et al., 2007), so it is more difficult for current to flow into the subsurface. This condition will lead to higher model errors produced from the inversion of electrical resistivity data obtained using flat base electrodes than peak electrodes. This effect can be minimized by applying conductive gel between the flat base electrodes and the concrete surface (Zouhri & Lutz, 2010; Putra et al., 2020). The gel is made of an electrolyte solution, which serves as an intermediary medium that improves the coupling and lowers the contact resistance. In addition, spraying saltwater on the concrete surface before applying the gel further decreases the contact resistance (Athanasiou et al., 2007). As a result, the current can flow more easily into the subsurface and minimize errors associated with data acquisition.

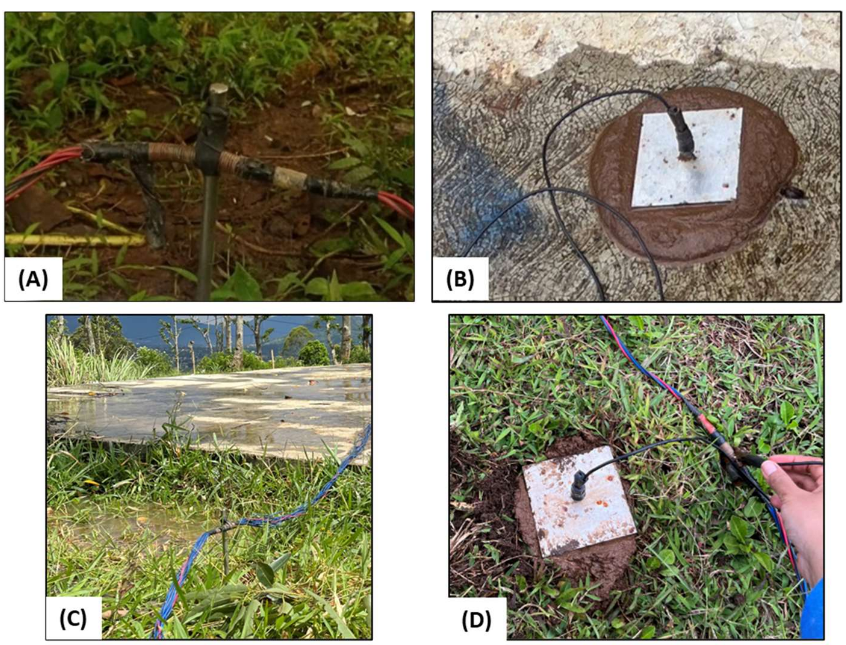

Figure 3. A peak electrode (A and C) and a flat base electrode (B and D). A peak electrode requires insertion into the soil, whereas a flat base electrode can be placed on top of the soil and the concrete surface.

2.2.2. Electrical Resistivity Method

The electrical resistivity method is an active and non-destructive geophysical method used for shallow exploration and determining subsurface layers up to depths of 300-500 m. This method can determine changes in resistivity values of rock layers beneath the surface by injecting DC current using electrodes. Ohm's law is the basis of the resistivity method (Loke, 1999), expressed by Equation 1 below.

$$R = \rho \frac{L}{A} \qquad (1)$$

where R is electrode resistance to subsurface materials (Ω), ρ indicates subsurface resistivity (Ωm). The magnitude of R is also directly proportional to the length L (m) and inversely proportional to the electrode's cross-sectional area A (m2). The resistivity is calculated by rearranging Equation 1 into Equation 2, which represents the apparent resistivity by assuming that the subsurface medium is homogeneous isotropic.

$$\rho_a = kR \qquad (2)$$

where ρ_a subsurface apparent resistivity and k represents the geometric factor of the electrode configuration. The apparent resistivity can be converted to the true resistivity of the subsurface using the inversion method. The resistance of peak and flat-base electrodes is influenced by their geometry (Dwight, 1936; Yuliadi et al., 2021). Therefore, Equation 2 can be modified to Equations 3 and 4 for peak and flat base electrodes.

$$\rho_a = kR \frac{2\pi l}{\ln\left(\frac{4l}{d}\right) - 1} \qquad (3)$$

$$\rho_a = kR \frac{2\pi l}{\ln\left(\frac{8w}{0.5w+t}\right) - 1} \qquad (4)$$

Where l indicates the length of peak and flat base electrodes (m), d is the diameter of peak electrodes (m), w represents the width of flat base electrodes (m), and t is the thickness of flat base electrodes (m).

2.2.3. Wenner-Alpha Configuration

The electrode configuration during the survey follows the Wenner-Alpha configuration, with the electrode spacing arranged in a specific pattern. The potential electrodes are situated between the current electrodes, where the distance between them is constant (P1C1 = P2C2 = a and P1C2 = P2C1 = 2a) (Telford et al., 1990), as shown in Figure 2. Wenner-Alpha configuration is sensitive to lateral changes and has reasonable vertical resolution (Reynolds, 1997). However, the penetration depth of the Wenner configuration is limited, making it suitable for shallow targets, such as identifying potential water leakage from a shallow water pool. In addition, this configuration has been shown to perform better against noisy data than the Wenner-Beta and Wenner-Gamma configurations (Oyeyemi et al., 2022).

The geometric factor for the Wenner-alpha configuration is $k = 2\pi a$, where a is the inter-electrode spacing (Figure 4). The geometric factor k is inserted into equations 3 and 4. Therefore, the equation for the apparent resistivity can be expressed by Equations 5 and 6 below for peak and flat-base electrodes, respectively.

$$\rho_a = 2\pi a R \frac{2\pi l}{\ln\left(\frac{4l}{d}\right) - 1} \qquad (5)$$

$$\rho_a = 2\pi a R \frac{2\pi l}{\ln\left(\frac{8w}{0.5w+t}\right) - 1} \qquad (6)$$

We assume that the electrical current emitted by a peak and flat base electrode can travel far in the subsurface before reaching other electrodes. Therefore, the geometry factor in Equations 5 and 6 has a minimum contribution to the measured apparent resistivity (ρ_a), which can be neglected (Mukmin et al., 2014). Athanasiou et al. (2007) shows that the model error from using peak or flat base electrodes with the same electrode configuration is comparable (the difference is 2.3% and no systematic bias). As a result, Equations 5 and 6 can be simplified into Equations 7 and 8.

$$\rho_a = 2\pi a R \quad (7)$$

$$\rho_a = 2\pi a \frac{\Delta V}{I} \quad (8)$$

where ΔV is the potential difference between the potential electrodes (V) and I represent the current injected by the current electrodes (A).

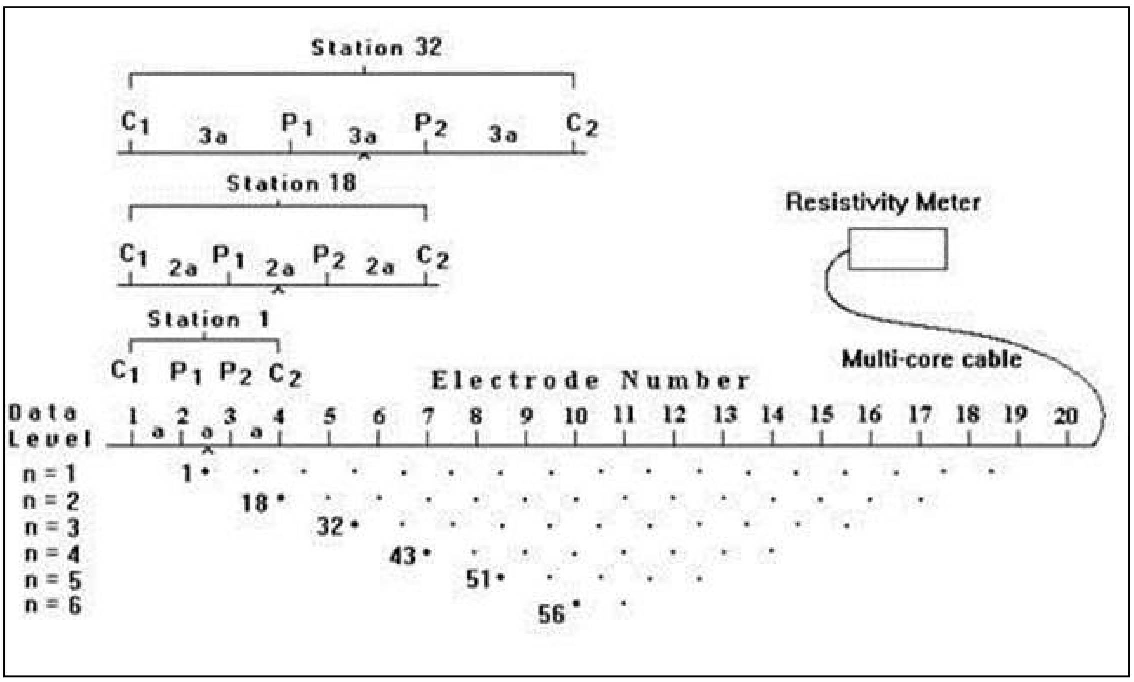

Figure 4. Wenner-Alpha configuration with a constant inter-electrode spacing (a) (Loke & Lane, 2004). The spacing increases for the following sequence of measurements by multiplying a with constant n to acquire the resistivity from a deeper subsurface to build a pseudosection. The maximum n-separation between electrodes is nmax.

2.2.4. Inversion Method

Inversion is a mathematical and statistical technique used to obtain information about a phenomenon based on observations of the system. The inversion is conducted to obtain a model perturbed for several iterations to get a close match between the model and field measurement data (Loke, 2022). In this study, the inversion method is performed to obtain the true resistivity of the subsurface from apparent resistivity using the least-square and robust constraint.

The least-square method is based on the smoothness-constrained least-square method embedded in Res2dinv software version 4.8.10 (deGroot-Hedlin & Constable, 1990; Loke et al., 2003; Sasaki, 1992), as shown by equation 9 and 10. This method adjusts the model by reducing the square difference between calculated and measured apparent resistivity values while also applying smoothness. A measure of the difference between data and the model (model error) is represented by the RMS error, updated over iterations until the RMS error does not change significantly as the iteration increases (equation 11). This method is preferentially used to invert the subsurface with gradual material boundaries or without sharp contacts (Grandis, 2009).

$$(J^T W_d^T W_d J + \lambda F)\Delta q_k = J^T W_d^T W_d g \qquad (9)$$

$$F = \alpha_x C_x^T C_x + \alpha_z C_z^T C_z \qquad (10)$$

$$q_{k+1} = q_k + \Delta q_k \qquad (11)$$

where J is a Jacobian matrix of partial derivatives, λ represents a damping factor, Δq_k indicates model resistivity change at k^{th} iteration, q_k is a model resistivity vector at k^{th} iteration, g is data misfit vector, W_d is a diagonal weighting metric that incorporates the effect of the data errors where data points with a smaller error are given larger weight in the inversion process, α represents a weight factor, C_x indicates horizontal roughness filters, and C_z is a vertical roughness vector.

The model obtained from the least-square method tends to have a smooth transition between resistivity values (Loke et al., 2003). The sharp boundary between the water pool and the soil will result in a transition in resistivity values from the well to the soil. Therefore, the robust constraint inversion method is also used. This method reduces the model error by decreasing the absolute difference between the measured and calculated apparent resistivity values (Abs. error), which works reasonably well for the data with outliers from non-random sources, such as operator mistakes or equipment problems. In this method, there is a cut-off factor that limits or controls the difference between the measurement data and the calculated data, leading to a sharper interface between different resistivity values. A detailed explanation of the inversion methods can be seen in the Res2Dinv manual, which is available for free.

3. Result and Discussion

3.1. Result

3.1.1. Inversion Result using Peak Electrodes

The inverted resistivity model from the Wenner-Alpha array with all peak electrodes is shown in Figure 5. The result shows a layered resistivity trend along the soil area for least-square and robust constraint models (Figure 5A, B). However, the model produced by the robust constraint method has a sharper transition of resistivity values than the least-square method.

It can also be seen that the models are quite different around the water pool, indicated by low resistivity values (Figures 5A, B). The robust constraint method results in a sharper transition from the water pool to the surrounding soil with a lower model error than the least-square method (7.3% vs 12.5%) (Figures 5A, B). A similar trend of model error is also shown by the L1 norm data misfit between measured and inverted apparent resistivity (Figures 5C, D). In addition, neither inversion method can resolve the water pool geometry, as shown by the vertical extent of the low resistivity values, which is larger than the pool thickness (2.15 m). This can be misinterpreted as leakage associated with cracks on the water pool surface.

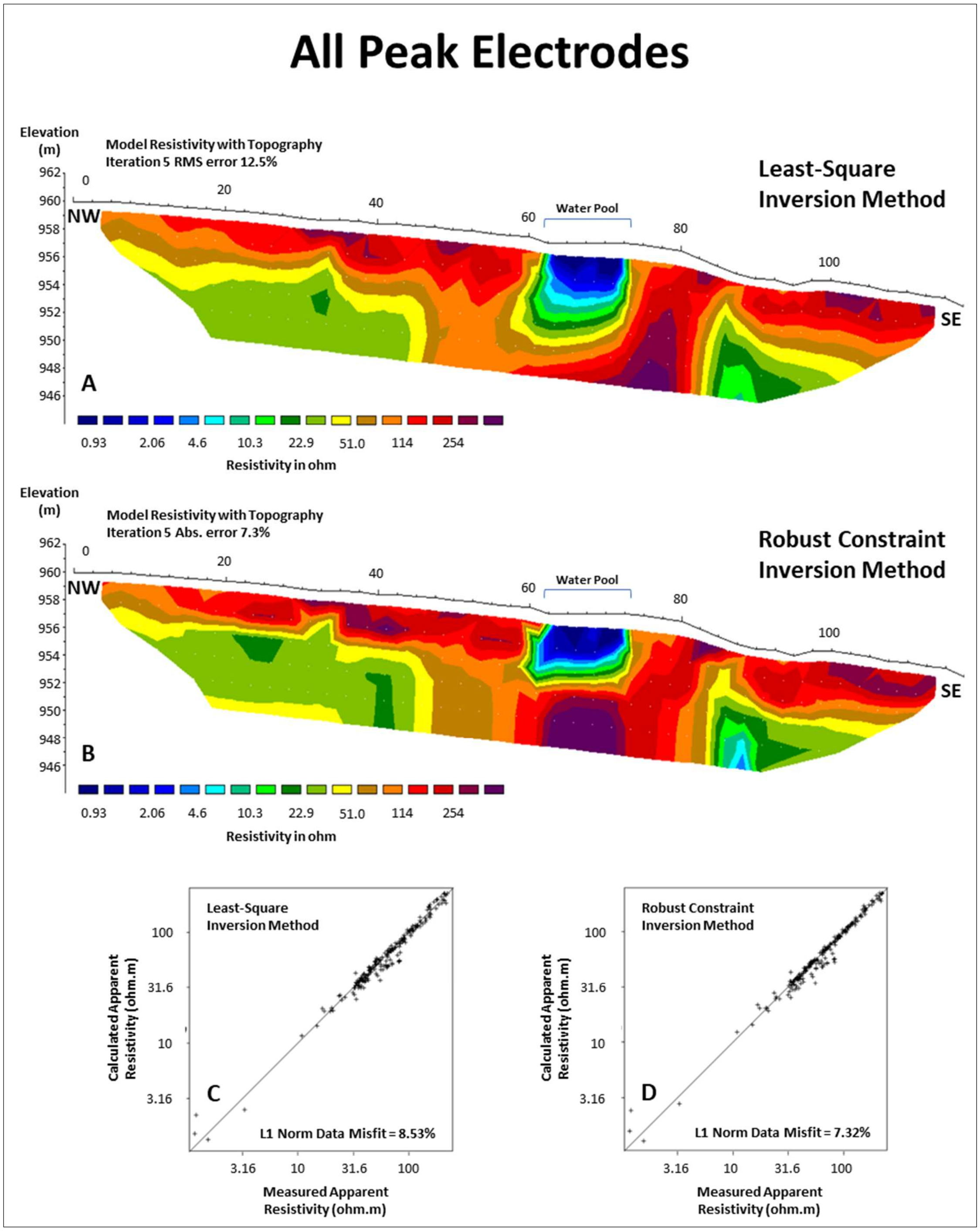

Figure 5. Inverted true resistivity models using least-square and robust constraint methods (A and B). These models were obtained from the Wenner-Alpha array using only peak electrodes applied to the soil. Cross plots of measured and calculated apparent resistivity from both inversion methods for all data points are also depicted that show a positive correlation, and the L1 norm data misfit for these plots is also shown (C and D)

3.1.2. Inversion Result using A Combination of Peak and Flat Base Electrodes

The inverted resistivity model from the Wenner-Alpha array with a combination of peak and flat base electrodes is shown in Figure 6. The results show a layered resistivity trend along the soil area for both models produced by the least-square and robust constraint methods (Figure 6A, B). However, the latter creates a sharper interface between the resistivity values with a smaller model error than the former (5.6% vs 14.4%). A similar trend of model error is also shown by the L1 norm data misfit (Figures 6C, D)

The location of the water pool can be observed in both models, identified by low resistivity values (Figure 6A, B). However, the vertical extent of the well inferred from the resistivity values is larger than the water pool thickness, which can be misinterpreted as leakage underneath the water pool. A smearing effect is also observed, shown by the extension of the low resistivity trend towards the peak electrodes in the Northwest from both inverted models (Figure 6).

3.1.3. Inversion Result using Flat Base Electrodes

The inverted resistivity model from the Wenner-Alpha array with all flat base electrodes is shown in Figure 7. The results indicate that both inversion methods produce a comparable layered resistivity trend along the soil area. However, the robust constraint produces a shaper transition between resistivity values compared to the least-square method (Figure 7A, B). The robust constraint method can also resolve the pool geometry (width = 10 m and thickness = 2 m), depicted by low resistivity surrounded by higher resistivity value associated with the soil (Figure 7B). In addition, the model error generated using the robust constraint method is lower than the least square method (3.4% vs 10.6%). A similar trend of model error is also shown by the L1 norm data misfit (Figures 5C, D).

3.2. Discussion

In 2D cross-sections inverted using the robust constraint method, the shape of the water pool is more apparent. This is because the robust constraint method is more sensitive to sharp contacts between interfaces of subsurface materials than the least-square method. Further analysis is conducted to compare the use of different combinations of electrode types inverted using the robust constraint method to determine if the geometry of the water pool is accurately resolved. The pool's geometry appears consistent with the field conditions in the cross-section using all flat base electrodes (Figure 6B). It is observed that the width and thickness of the water pool are 10 m and 2 m, respectively. These values are comparable with the actual width and thickness of the pool (10.8 m and 2.15 m) (Section 3). Furthermore, the extent of low resistivity values in the model is content within the pool. This indicates that no leakage occurs underneath the pool. This inversion result is robust because the flat base electrodes can transmit and receive electrical currents on the concrete surface, which cannot be achieved with peak electrodes. In the case of the concrete surface where peak electrodes are not inserted, some data points will be missing and filled with dummy values during data processing. The dummy data points are extrapolated to the right and left sides of the water pool where data points are present, resulting in mismatched data points with the actual field geometry. In addition, the robust constraint method applied to flat base electrodes yields the smallest L1 norm data misfit (Table 1).

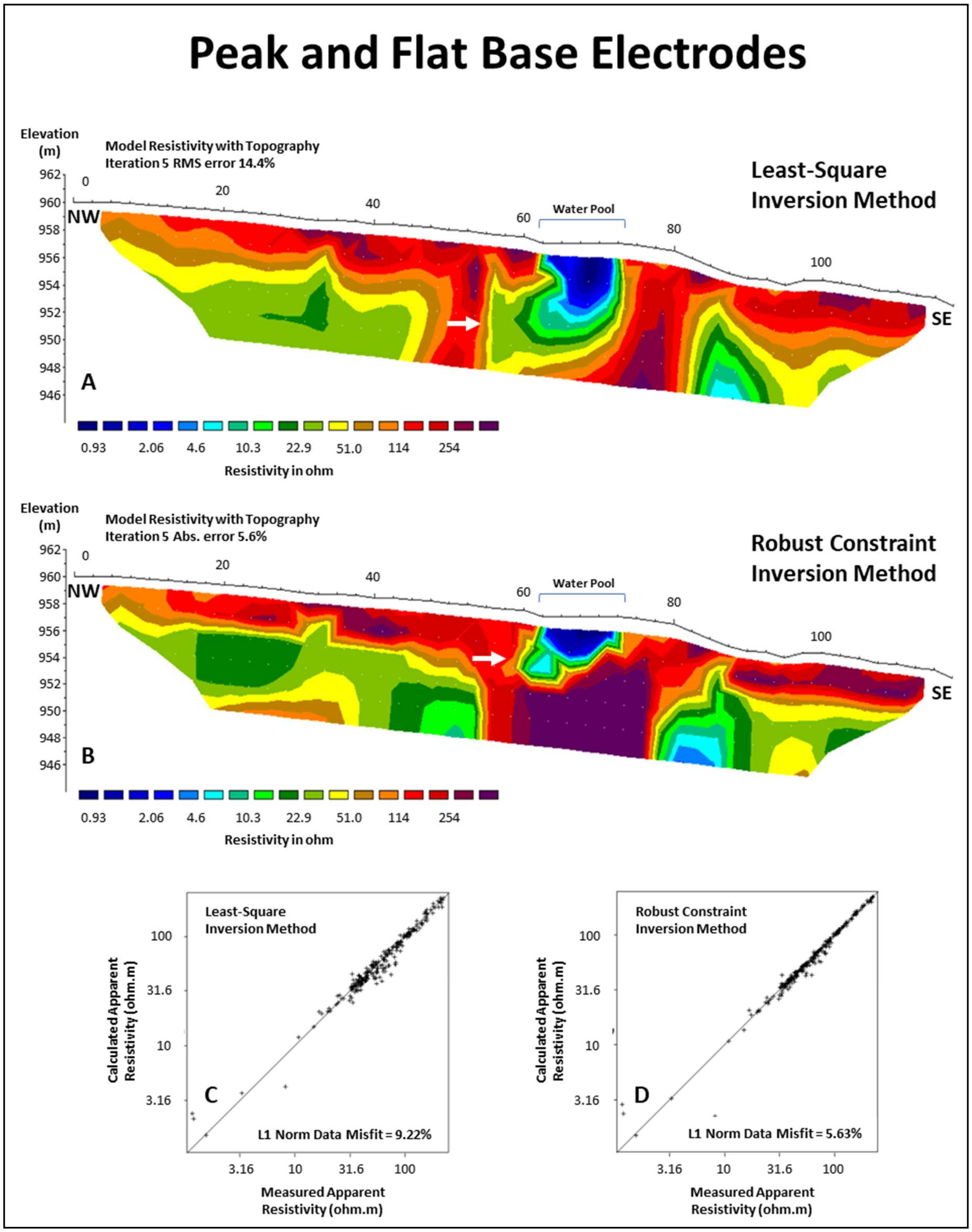

Figure 6. Inverted true resistivity model using least-square and robust constraint methods (A and B). These models were obtained from the Wenner-Alpha array using peak and flat-base electrodes. Smearing effects are shown by white arrows. Cross plots of measured and calculated apparent resistivity from both inversion methods are also depicted, which shows a positive correlation (C and D). The L1 norm data misfit for these plots is also shown (C and D).

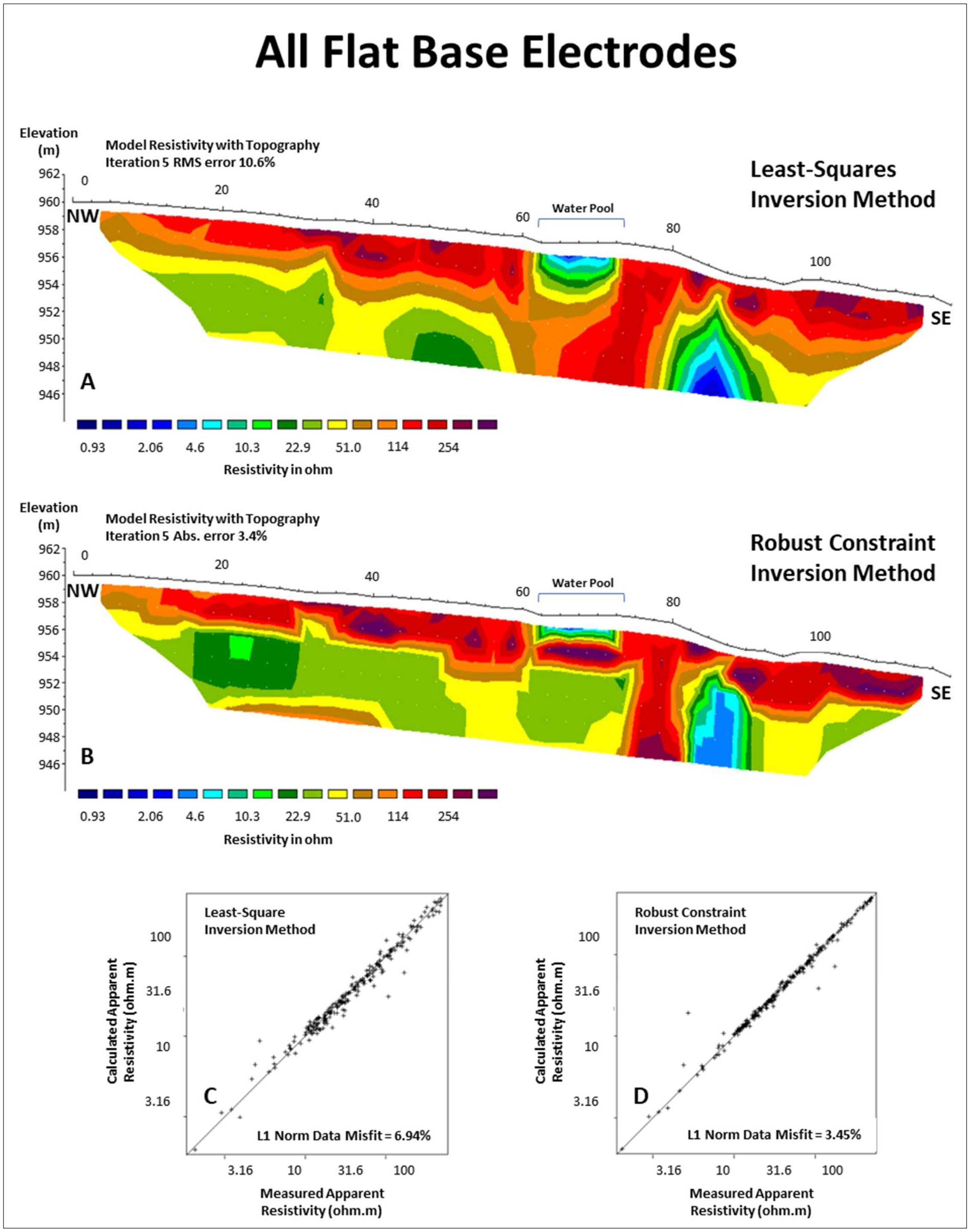

Figure 7. Inverted true resistivity model using least-square and robust constraint methods (A and B). These models were obtained from the Wenner-Alpha array using only flat base electrodes. Cross plots of measured and calculated apparent resistivity from both inversion methods for all data points are also depicted, which show a positive correlation (C and D). The L1 norm data misfit for these plots is also shown (C and D).

Table 1. A summary of L1 norm data misfit between the measured and calculated resistivity values for three combinations of peak and flat base electrodes, inverted using the robust and least-square methods.

Method	Error (%)	
	Robust	Least-Square
Peak	7.32	8.53
Peak and Flat	5.63	9.22
Flat	3.45	6.94

The L1 norm data misfit obtained from the robust constraint method using all flat base electrodes is 3.45%, whilst using all peak electrodes yields 6.94 %. This contrasts a previous study (Athanasiou et al., 2007), which shows that all flat base electrodes give a higher misfit than all peak electrodes. We argue that the misfit from using all flat base electrodes is smaller due to several reasons. (1) The environments in this study are less complex, which is layered soil. (2) The contact resistance between flat base electrodes and the concrete surface that covers the well is reduced by applying electrolyte gel. (3) Flat base electrodes can cover both soil and concrete surface, leading to full coverage in the survey line, preventing missing data points.

In this study, we neglect the influence of electrode shape (peak and flat) on the inversion results. However, the results from a combination of peak and flat base electrodes are very different from all flat base electrodes. This occurs because the inversion methods (least-square and robust constraint) use weighting based on the error value, where a higher weight factor is assigned to the resistivity data that provides a lower error. In this case, the lower error comes from flat base electrodes than peak electrodes due to smaller contact resistance because of the added electrolyte gel. This also leads to a smearing effect in the inversion result (Figure 6).

The water pool is buried to a depth of 2.15 meters, with its top visible at the surface. This shallow burial depth exposes the water pool structure to limited pressure from the surrounding soil and negligible temperature gradients, making leakage from these factors unlikely. However, Kiara Payung is situated in West Java, a seismically active region experiencing both shallow and deep earthquakes (Supendi et al., 2018; Ashadi & Kaka, 2019). Seismic waves from these earthquakes can travel through the weathered soil surrounding the pool, generating significant ground motion that can affect the pool's structure and potentially cause leakage. Therefore, we recommend conducting additional electrical resistivity surveys using flat base electrodes to monitor for potential leakage effectively.

4. Conclusion

This study is conducted to detect a potential leakage underneath a water pool located at Kiara Payung, Sumedang, West Java, using the electrical resistivity method with peak and/or flat base electrodes. There are several conclusions from this study.

a). Flat base electrodes are suitable for use on a hard surface, such as a concrete surface that covers the well without causing damage to its structure.

b). Modelling results indicate that the robust constraint method produces a sharp contact between resistivity values. This leads to a more robust model water pool geometry than the least-square inversion method.

c). The model obtained from the robust constraint method using all flat base electrodes yields the best result in resolving the well geometry. It also produces the smallest model error and L1 norm misfit. The best modelling result using the robust constraint method with all flat base electrodes indicates that no leakage occurs underneath the water pool, as shown by the low resistivity values inside the pool.

Acknowledgement
We acknowledge the Hibah Publikasi Terindeks Internasional (PUTI) Q2 NOMOR: NKB-733/UN2.RST/HKP.05.00/2023 from Universitas Indonesia, which the corresponding author receives. The author would also like to thank PT. Geoscan Eksplorasindo, which provides the electrical resistivity measurement tool. We appreciate Aep Saepudin, Asep, Rifdan Hilmi, and Victo, who assist in data acquisition. In addition, we thank Dr. Eng. Supriyanto, M.Sc, Dr. Muhammad Bisri Mustofa, M.Si, and Iskadarsyah, M.Si for their suggestions on the final version of this manuscript.

References
Adhe, A., Waterman, & Nurkhamin. (2022). Perbandingan Hasil Deteksi Air Tanah Dengan Metode Geolistrik Konfigurasi Schlumberger, Wenner, Wenner-Schlumberger, Dipole- Dipole Dan Pole-Pole. Prosiding Nasional Rekayasa Teknologi Industri Dan Informasi XVII Tahun 2022 (ReTII), 132-139.

Ashadi, A. L., & Kaka, S. I. (2019). Ground-Motion Relations for Subduction-Zone Earthquakes in Java Island, Indonesia. *Arabian Journal for Science and Engineering*, *44*(1), 449–465. https://doi.org/10.1007/s13369-018-3563-x

Athanasiou, E. N., Tsourlos, P. I., Vargemezis, G. N., Papazachos, C. B., & Tsokas, G. N. (2007). Non-destructive DC resistivity surveying using flat-base electrodes. In Near Surface Geophysics (Vol. 5, Issue 4, pp. 263–272). European Association of Geoscientists & Engineers. https://doi.org/10.3997/1873-0604.2007008

Carrara, E., Carrozzo, M. T., Fedi, M., Florio, G., Negri, S., Paoletti, V., Paolillo, G., Quarta, T., Rapolla, A., & Roberti, N. (2001). Resistivity and Radar surveys at the Archaeological site of Ercolano. Journal of Environmental and Engineering Geophysics, 6(3), 123–132. https://doi.org/10.4133/JEEG6.3.123

Chabaane, A., Redhaounia, B., & Gabtni, H. (2017). Combined application of vertical electrical sounding and 2D electrical resistivity imaging for geothermal groundwater characterization: Hammam Sayala hot spring case study (NW Tunisia). Journal of African Earth Sciences, 134, 292–298. https://doi.org/10.1016/j.jafrearsci.2017.07.003

deGroot-Hedlin, C., & Constable, S. (1990). Occam's inversion to generate smooth, two-dimensional models from magnetotelluric data. GEOPHYSICS, 55(12), 1613–1624. https://doi.org/10.1190/1.1442813

Dwight, H. B. (1936). Calculation of Resistances to Ground. Transactions of the American Institute of Electrical Engineers, 55(12), 1319–1328. https://doi.org/10.1109/T- AIEE.1936.5057209

Grandis, H. (2009). Pengantar Pemodelan Inversi Geofisika. Himpunan Ahli Geofisika Indonesia (HAGI).

Karavul, C., Karaaslan, H., & Demirkol, A. (2016). Investigation of structures in the Alabanda Bouleuterion by electrical resistivity method. Arabian Journal of Geosciences, 9(7), 511. https://doi.org/10.1007/s12517-016-2535-2

Kurniawan, M. F., Koesuma, S., & Darsono. (2017). Perbandingan Elektroda Konvensional dan Elektroda Tempel pada Metode Resistivitas untuk Identifikasi Model Anomali Bawah Permukaan. Prosiding Pertemuan Ilmiah XXXI HFI Jateng & DIY, 33-37.

Loke, M. H. (1999). Electrical Imaging Surveys for Environmental and Engineering Studies: A Practical Guide to 2D and 3D Surveys. 2, 70.

Loke, M. H. (2022). Tutorial: 2D and 3D Electrical Imaging Surveys. www.geotomofost.com.
Loke, M. H., Acworth, I., & Dahlin, T. (2003). A comparison of smooth and blocky inversion methods in 2D electrical imaging surveys. Exploration Geophysics, 34(3), 182–187. https://doi.org/10.1071/EG03182

Loke, M. H., & Lane, J., John W. (2004). Inversion of Data from Electrical Resistivity Imaging Surveys in Water-Covered Areas. Exploration Geophysics, 35(4), 266–271. https://doi.org/10.1071/EG04266

Mohamaden, M. I. I., Hamouda, A. Z., & Mansour, S. (2016). Application of electrical resistivity method for groundwater exploration at the Moghra area, Western Desert, Egypt.The Egyptian Journal of Aquatic Research, 42(3), 261–268. https://doi.org/10.1016/j.ejar.2016.06.002

Mukmin, M., Kali, A., & Mukhlis, B. (2014). Perbandingan Nilai Tahanan Pertanahan Pada Area Reklamasi Pantai (Citraland). Jurnal Metrik, 1(1).

Oyeyemi, K. D., Aizebeokhai, A. P., Metwaly, M., Omobulejo, O., Sanuade, O. A., & Okon, E. E. (2022). Assessing the suitable electrical resistivity arrays for characterization of basement aquifers using numerical modeling. Heliyon, 8(5), e09427. https://doi.org/10.1016/j.heliyon.2022.e09427

Putra, F. D., Paembonan, Y., & Rizki, R. (2020). Aplikasi Metode Flat Base Electrical Resistivity Survey Untuk Mengetahui Kerusakan di Jalan Terusan Ryacudu Lampung Selatan. Jurnal Geosaintek, 6(3). http://dx.doi.org/10.12962/j25023659.v6i3.7890

Ramirez, A., Daily, W., Binley, A., LaBrecque, D., & Roelant, D. (1996). Detection of Leaks in Underground Storage Tanks Using Electrical Resistance Methods. *Journal of Environmental and Engineering Geophysics*, *1*(3), 189–203. https://doi.org/10.4133/JEEG1.3.189

Reynolds, J. M. (1997). An Introduction to Applied and Environmental Geophysics. Chichester: John Wiley and Sons Ltd.

Riwayat, A. I., Ahmad Nazri, M. A., & Zainal Abidin, M. H. (2018). Application of Electrical Resistivity Method (ERM) in Groundwater Exploration. Journal of Physics: Conference Series, 995(1), 012094. https://doi.org/10.1088/1742-6596/995/1/012094

Sasaki, Y. (1992). Resolution of Resistivity Tomography Inferred from Numerical Simulation. In Geophysical Prospecting (Vol. 40, Issue 4, pp. 453–463). European Association of Geoscientists & Engineers. https://doi.org/10.1111/j.1365-2478.1992.tb00536.x

Supendi, P., Nugraha, A. D., Puspito, N. T., Widiyantoro, S., & Daryono, D. (2018). Identification of active faults in West Java, Indonesia, based on earthquake hypocenter determination, relocation, and focal mechanism analysis. *Geoscience Letters*, *5*(1), 31. https://doi.org/10.1186/s40562-018-0130-y

Telford, W. M., Geldart, L. P., & Sheriff, R. E. (1990). Applied Geophysics Second Edition. Melbourne: Cambridge University.

Yuliadi, H., Hardi, S., & Rohana, R. (2021). Analisis Perbandingan Tahanan Pentanahan Pada Elektroda Batang Dan Plat Untuk Perbaikan Nilai Resistansi Pembumian. Jurnal Teknik Elektro, 4(1). https://doi.org/DOI: https://doi.org/10.30596/rele.v4i1.7828

Zouhri, L., & Lutz, P. (2010). A comparison of peak and plate electrodes in electrical resistivity tomography: Application to the chalky groundwater of the Beauvais aquifer (northern part of the Paris basin, France). Hydrological Processes, 24(21), 3040–3052. https://doi.org/10.1002/hyp.7719s